J Neurophysiol 93: 2194–2232, 2005.
First published November 3, 2004; doi:10.1152/jn.00983.2004.

Single-Column Thalamocortical Network Model Exhibiting Gamma Oscillations, Sleep Spindles, and Epileptogenic Bursts

Roger D. Traub,[1] Diego Contreras,[2] Mark O. Cunningham,[3] Hilary Murray,[3] Fiona E. N. LeBeau,[3] Anita Roopun,[3] Andrea Bibbig,[1] W. Bryan Wilent,[2] Michael J. Higley,[2] and Miles A. Whittington[3]

[1]*Departments of Physiology and Pharmacology, and Neurology, State University of New York, Downstate Medical Center, Brooklyn, New York;* [2]*Department of Neuroscience, University of Pennsylvania School of Medicine, Philadelphia, Pennsylvania; and* [3]*School of Biomedical Sciences, University of Leeds, Leeds, United Kingdom*

Submitted 20 September 2004; accepted in final form 3 November 2004

Traub, Roger D., Diego Contereas, Mark O. Cunningham, Hilary Murray, Fiona E. N. LeBeau, Anita Roopun, Andrea Bibbig, W. Bryan Wilent, Michael Higley, and Miles A. Whittington. Single-column thalamocortical network model exhibiting gamma oscillations, sleep spindles, and epileptogenic bursts. *J Neurophysiol* 93: 2194–2232, 2005. First published November 3, 2004; doi:10.1152/jn.00983.2004. To better understand population phenomena in thalamocortical neuronal ensembles, we have constructed a preliminary network model with 3,560 multicompartment neurons (containing soma, branching dendrites, and a portion of axon). Types of neurons included superficial pyramids (with regular spiking [RS] and fast rhythmic bursting [FRB] firing behaviors); RS spiny stellates; fast spiking (FS) interneurons, with basket-type and axoaxonic types of connectivity, and located in superficial and deep cortical layers; low threshold spiking (LTS) interneurons, which contacted principal cell dendrites; deep pyramids, which could have RS or intrinsic bursting (IB) firing behaviors, and endowed either with nontufted apical dendrites or with long tufted apical dendrites; thalamocortical relay (TCR) cells; and nucleus reticularis (nRT) cells. To the extent possible, both electrophysiology and synaptic connectivity were based on published data, although many arbitrary choices were necessary. In addition to synaptic connectivity (by AMPA/kainate, NMDA, and $GABA_A$ receptors), we also included electrical coupling between dendrites of interneurons, nRT cells, and TCR cells, and—in various combinations—electrical coupling between the proximal axons of certain cortical principal neurons. Our network model replicates several observed population phenomena, including *1*) persistent gamma oscillations; *2*) thalamocortical sleep spindles; *3*) series of synchronized population bursts, resembling electrographic seizures; *4*) isolated double population bursts with superimposed very fast oscillations (>100 Hz, "VFO"); *5*) spike-wave, polyspike-wave, and fast runs (about 10 Hz). We show that epileptiform bursts, including double and multiple bursts, containing VFO occur in rat auditory cortex in vitro, in the presence of kainate, when both $GABA_A$ and $GABA_B$ receptors are blocked. Electrical coupling between axons appears necessary (as reported previously) for persistent gamma and additionally plays a role in the detailed shaping of epileptogenic events. The degree of recurrent synaptic excitation between spiny stellate cells, and their tendency to fire throughout multiple bursts, also appears critical in shaping epileptogenic events.

INTRODUCTION

The greatest scientific challenge, perhaps, in all of brain research is how to understand the cooperative behavior of large numbers of neurons. Such cooperative behavior is necessary for sensory processing and motor control, planning, and in the case of humans, at least, for thought and language. Yet it is a truism to observe that single neurons are complicated little machines, as well as to observe that not all neurons are alike—far from it; and finally to observe that the connectional anatomy and synaptology of complex networks, in the cortex for example, have been studied long and hard, and yet are far from worked out. Any model, even of a small bit of cortex, is subject to difficulties and hazards: limited data, large numbers of parameters, criticisms that models with complexity comparable to the modeled system cannot be scientifically useful, the expense and slowness of the necessary computations, and serious uncertainties as to how a complex model can be compared with experiment and shown to be predictive.

The above difficulties and hazards are too real to be dismissed readily. In our opinion, the only way to proceed is through a state of denial that any of the difficulties need be fatal. The reader must then judge whether the results, preliminary as they must be, help our understanding.

Previous models of cortical or thalamocortical circuits have been developed, usually with specific applications in mind (Bal et al. 2000; Bazhenov et al. 2002, 2004; Bush and Sejnowski 1996; Contreras et al. 1996; Destexhe et al. 1996, 1999; Douglas and Martin 1991; Golomb and Amitai 1997; Lytton et al. 1997; Pinto et al. 2003; Wang and Rinzel 1993). These previous models tend to use small numbers of cells and usually represent each cell with one or a few compartments. We are not aware of a previous model that has a multiplicity of cell types and firing behaviors in cortical cells, including regular spiking (RS), fast rhythmic bursting (FRB) (Gray and McCormick 1996; Steriade et al. 1998), and intrinsic bursting (IB) (McCormick et al. 1982; Nowak et al. 2003). It has been unusual to include electrical coupling, particularly between the axons of principal cells, a form of coupling that appears to be essential for persistent gamma and for very fast oscillations (>70 Hz) (Cunningham et al. 2004a,b; Traub et al. 2002, 2003a,b).

We have attempted here to construct a thalamocortical circuit model that has applicability to the study of a range of emergent behaviors in the thalamocortical network. Our attempt hinges on an effort to be faithful to a range of intrinsic properties in different neuronal types (Llinás 1988) and to

Address for reprint requests and other correspondence: R. D. Traub at Departments of Physiology and Pharmacology, and Neurology, State University of New York, Downstate Medical Center, 450 Clarkson Ave., Box 31, Brooklyn, NY 11203 (E-mail: roger.traub@downstate.edu).

The costs of publication of this article were defrayed in part by the payment of page charges. The article must therefore be hereby marked "*advertisement*" in accordance with 18 U.S.C. Section 1734 solely to indicate this fact.

include a variety of between-cell interactions, both chemical synaptic and gap junction-mediated. Although the model does indeed describe, predictively, several sorts of network behaviors (as will be seen below), it is insufficient to describe many others: for reasons that include, but are not limited to, the omission of many cell types, the requirement to make many guesses about structural details, the absence of mechanisms to simulate synaptic plasticity (either short-term or long-term), and the restriction of the model to a single column. In particular, the present model is best suited to address the physiology of network oscillations and epileptogenesis.

A major question to be addressed here concerns the role of axonal gap junctions (Schmitz et al. 2001) in epilepsy. A number of experimental studies suggest a role of gap junctions in epileptogenesis (Gajda et al. 2003; Jahromi et al. 2002; Köhling et al. 2001; Pais et al. 2003; Perez-Velazquez et al. 1994; Ross et al. 2000; Schweitzer et al. 2000; Szente et al. 2002; Traub et al. 2001, 2002). Earlier modeling studies of hippocampal pyramidal cell networks (Traub et al. 1999) predicted that gap junctions, if located between the axons of pyramidal cells, are expected to have 2 effects on epileptogenesis: *1*) they would lower the extent of recurrent chemical synaptic excitation required for population synchronization of bursts of action potentials; *2*) they would introduce a very fast oscillation (>70 Hz, "VFO") on top of the interictal field potential. [Earlier studies of such a superimposed very fast oscillation in hippocampus (Snow and Dudek 1984) had considered the possibility of field-effect–induced synchronization.] In the cortex, VFO is of interest not only because of its association with human epilepsy (Bragin et al. 1999; Staba et al. 2004), but also because of the appearance of VFO in somatosensory evoked potentials in rat barrel cortex (Jones and Barth 1999, 2002; Jones et al. 2000).

We have paid particular attention to electrical coupling between principal cell axons because of the necessity to include such an effect, to account for experimental recordings of kainate-induced persistent gamma in superficial layers of auditory cortex in vitro (Cunningham et al. 2004), and also because of clinical data documenting, in human epilepsy patients, the presence of VFO superimposed on seizure burst complexes, and on interictal spikes (Traub et al. 2001): earlier work in hippocampus (Traub and Bibbig 2000) had shown that the postulate of axonal coupling between hippocampal pyramidal cells could account for the occurrence of VFO on top of physiological sharp waves (Ylinen et al. 1995), even though the sharp waves are primarily mediated by a synaptically coupled network. Further details suggesting that axonal coupling could occur in cortex are discussed in APPENDIX B.

Topics covered in this paper include: kainate-induced persistent gamma oscillations and sleep spindles; then epileptogenesis, with illustrations of patterns resembling interictal spikes, fast runs, spike-wave, and polyspike-wave. These topics were selected because they are logically related: they are all associated with slow sleep oscillations, and its transition to seizures, in vivo (Steriade 2003). We include some experimental recordings that are consistent with some of the model predictions, particularly on the presence of very fast oscillations superimposed on epileptiform field potentials, and on firing patterns of layer 4 spiny stellate cells during seizurelike events. Further topics are considered in the appendices. APPENDIX A describes how individual cell types were modeled. APPENDIX B describes between-cell interactions, both synaptic and by electrical coupling. APPENDIX C deals with technical issues of how the large computations were carried out.

A note on terminology: sleep spindles refer to a well-known in vivo population phenomenon (Steriade 2001, 2003), appearing in natural slow-wave sleep in addition to other states, and consisting of cellular oscillations (about 10 to about 15 Hz, depending on species) that involve thalamic relay cells, nucleus reticularis thalami (nRT) cells, and cortical cells. Network phenomena in vitro, which exhibit a similar appearance in terms of cellular oscillations, shall be called simply "spindles."

METHODS

Simulation methods

We confine ourselves here to general comments on our philosophy of modeling and the overall network architecture. Specific details on single-cell properties are described in APPENDIX A; on synaptic and gap-junctional interactions (connectivity, kinetics, and conductance amplitudes) in APPENDIX B; and on programming issues and the use of the parallel computer in APPENDIX C. [In addition, interested readers may obtain copies of the Fortran code and Linux compilation and execution scripts by writing to roger.traub@downstate.edu.]

The approach to modeling single neurons grew out of 2 earlier studies (Traub et al. 1994, 2003c). The code described in the latter reference was the basis for simulating 2 of the cell types here. The approach is to use an electrotonic architecture containing dozens of compartments, but nowhere near the number of compartments used to model an anatomically reconstructed neuron. Network simulations, on a large scale anyway, are not practical with such detailed neurons. Dozens of compartments are sufficient to capture certain aspects of neuronal function, including differences in electrogenesis between axon, soma, and dendrites; action potential initiation in the axon; dendritic calcium spikes and bursts; spike backpropagation; and to allow for axons and/or dendrites to be electrically coupled between neurons.

The structure of a particular neuron is described by its compartmental topology; the values of electrotonic parameters such as specific membrane capacitance, membrane resistivity, and internal resistivity (some of which can be different in the axon compared with soma/dendrites); the densities of a fixed repertoire of ionic conductances, where the same repertoire of conductances was used, for the sake of simplicity, in *all* cell types; and by parameters describing the kinetics of $[Ca^{2+}]$ concentration in a thin submembrane shell. Again for the sake of simplicity, the first-order kinetic scheme for submembrane $[Ca^{2+}]$ concentration was the same for all cell types; only the particular parameters were different. Submembrane $[Ca^{2+}]$ concentration is used to gate the slow AHP conductance, and (along with membrane voltage) one of the fast K conductances—the "C" conductance. All neurons of a given type (e.g., layer 2/3 RS pyramidal neurons) have the same parameter set: heterogeneity can be introduced by the use of slightly different bias currents. A final simplification is to use, wherever possible, identical kinetics for voltage-sensitive channels between different neuron types. Exceptions to this latter rule include the use of different fast g_{Na} and delayed rectifier $g_{K(DR)}$ kinetics in pyramidal cells versus cells with stellate or interneuron-like morphology; and the use of different T-channel kinetics in nRT versus thalamocortical relay (TCR) neurons. Our experience has been that using 50 to 100 or so compartments is sufficient to capture many detailed aspects of neuronal firing behavior (Traub et al. 1994, 2003c).

The "standard repertoire" of active ionic conductances are these: fast, transient, g_{Na}; persistent g_{Na}; K conductances of delayed rectifier, A (transient, inactivating), slow AHP, C (fast voltage- and calcium-

dependent), "K2," and "M" types; high- and low-threshold g_{Ca}; and a relatively slow anomolous rectifier, or "h," conductance.

The cell types and cell locations of the 3,560-neuron model are shown in Fig. 1. The cortical portion of the model is one-dimensional, the dimension being cortical depth: dimensions parallel to the pia are not represented, so that the structure can be thought of as a column. Space is not defined within the thalamic portion. The reader should note the following: there is no layer 1; layers 2 and 3 are lumped together; a large variety of neuronal types are omitted, including but not limited to: neurogliaform cells, double bouquet cells, multipolar bursting neurons (Blatow et al. 2003), and numerous other sorts of interneurons; there are no pyramidal cells in layer 4; synaptic inhibition in layer 4 derives primarily from deep interneurons; there are no FRB cells in deep layers nor FRB interneurons (which were shown to exist by Steriade et al. 1998); there is homogeneity of cell structure within layers. Considerations in choosing the repertoire that we used were these: we began with a model of layer 2/3 circuitry that included RS and FRB pyramidal cells, as well as superficial fast-spiking (FS) and low-threshold spiking (LTS) interneurons (Cunningham et al. 2004a). We needed layer 4 stellate cells as the major recipient of thalamic inputs. Tufted pyramids in layer 5 are a major neuronal type, much studied, and important for cortical outputs not headed for the thalamus; and both IB and occasionally RS firing patterns have been described in these cells (Williams and Stuart 1999). Layer 6 pyramids were needed as an interface to the thalamus. Deep interneurons were necessary because, for among other reasons, we know that in vitro gamma/beta oscillations have different structure in deep versus superficial layers (A. Roopun and M. A. Whittington, unpublished data). Finally, both nRT and TCR thalamic neurons are essential for the understanding of thalamic oscillations, including sleep spindles, as presented here, but also for subsequent work including delta waves and the slow (<1 Hz) oscillation of sleep (Steriade et al. 1993).

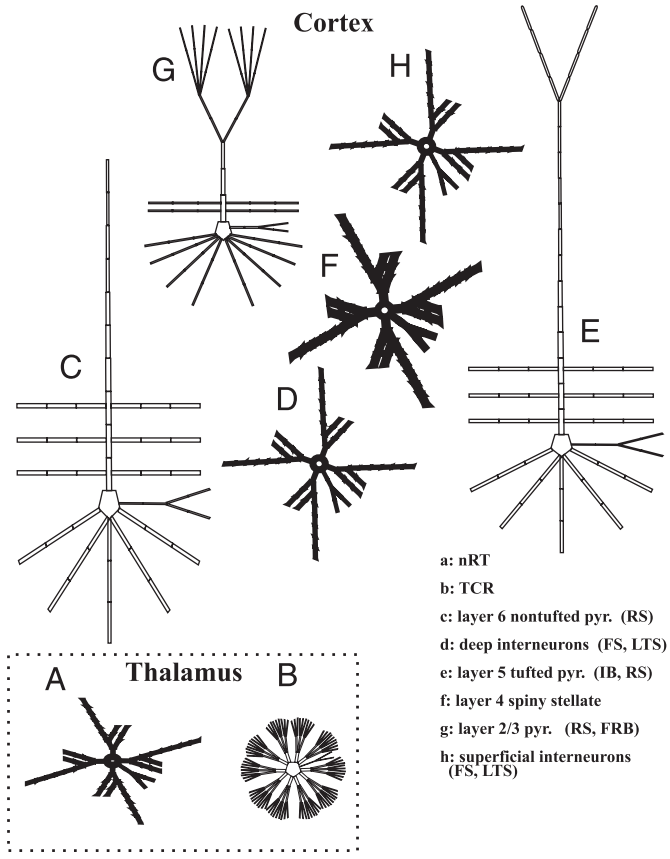

FIG. 1. General architecture of the model. All neurons are multicompartmental, with soma, branching dendrites, and a short branching axon. *Thalamic* portion of the network contains (a) 100 nucleus reticularis thalami (nRT) cells [each with low-threshold g_{Ca}, and lacking intrinsic gamma oscillatory properties (Contreras et al. 1993; Pinault and Deschênes 1992)], as well as (b) 100 "typical" thalamocortical relay (TCR) cells [i.e., also lacking intrinsic gamma oscillations (Steriade et al. 1993)]. *Cortical* portion contains the following cell types: (c) 500 layer 6 nontufted pyramidal neurons that connect intracortically, as well as to nRT and TCR neurons (the only model cortical cells to connect to the thalamus); (d) 100 deep fast-spiking (FS) basket interneurons, 100 deep axoaxonic interneurons, 100 deep low threshold spiking (LTS) dendrite-contacting interneurons; (e) 800 layer 5 tufted intrinsic bursting (IB) pyramidal neurons and 200 layer 5 tufted regular spiking (RS) pyramidal neurons; (f) 240 layer 4 spiny stellate cells, the major (but not only) recipients of thalamic inputs; (g) 1,000 layer 2/3 RS pyramidal cells and 50 layer 2/3 fast rhythmic bursting (FRB) pyramidal cells; (h) 90 superficial basket interneurons, 90 superficial axoaxonic interneurons, and 90 LTS interneurons.

APPENDIX A provides further details on the structure of the individual cell models and illustrates examples of some of their firing behaviors, considered as single neurons in isolation from other neurons.

The neurons were connected together *1*) by chemical synapses, using AMPA and NMDA receptors, and γ-aminobutyric acid-A ($GABA_A$; but not $GABA_B$) receptors; and *2*) gap junctions, that were nonrectifying and voltage-independent. Connections of both sorts were "wired up" randomly, subject to constraints on how many connections there were, and the possible locations of postsynaptic compartments. A given excitatory synapse activated both α-amino-3-hydroxy-5-methyl-4-isoxazolepropionic acid (AMPA) and *N*-methyl-D-aspartate (NMDA) receptors. Gap junctions were located between dendrites of cortical interneurons, of nRT cells (Landisman et al. 2002), and of TCR cells (Hughes et al. 2002a). Gap junctions could also be located between the axons of *1*) the pool of superficial pyramids, RS and FRB; and/or *2*) the pool of spiny stellates; and/or *3*) the pool of layer 5 tufted pyramids; and/or *4*) the pool of layer 6 nontufted pyramids. It was a major assumption that only homologous sorts of glutamatergic neurons could be electrically coupled by their axons (see APPENDIX B).

We justified the use of axonal coupling as follows: *1*) it is necessary in models for the occurrence of gamma oscillations (Cunningham et al. 2004a); *2*) spikelets occur in cortical neurons (Cunningham et al. 2004a; Deschênes,1981; Thomson and Bannister 2004; however, the Deschênes study attributed the spikelets to synaptic activation); *3*) there is staining for pannexin 2 [a putative component of the electrical coupling substrate between axons (Bruzzone et al. 2003)] throughout cortical layers 2–6 (Cunningham et al. 2004a); *4*) very fast oscillations occur in the cortex (Traub et al. 2001; this paper).

Certain important state variables could not be included, such as fluctuations in extracellular ion concentrations. In addition, we did not allow for afferent inputs (coming from outside the model network), or for specific effects of neuromodulators on membrane properties, although we did depolarize selected neuronal subpopulations (including FRB neurons, and at times pyramidal neurons in layers 5 and 6), using steady bias currents. All collective behaviors simulated are thus essentially "autonomous" in the model network.

The effects of the many simplifications made here will become known as progressively more detailed models are constructed and their behaviors analyzed. It is to be hoped that—as the model incorporates further cell types, membrane currents, metabotropic effects, more accurate synaptic connectivity, and so forth—then it will be possible to study a broader range of network phenomena, including the slow oscillation of sleep, gamma oscillations in deep cortical layers, and cortical responses to thalamic activation.

In APPENDIX B, we list the set of "baseline" synaptic conductance scaling constants. These, and details of connectivity, were arrived at after extensive (dozens) of preliminary simulations. (Many dozens of preliminary simulations were also necessary for each individual cell model.) Then, for this paper, we can list modifications in synaptic conductances relative to the baseline values. APPENDIX B also describes between-cell connectivity (synaptic and gap junctional), methods for

estimating field potentials, and other matters related to ensemble activity.

APPENDIX C describes computer science and numerical integration aspects of how our large calculations were performed on a parallel computer (Linux cluster). (For questions about these issues and copies of the code, or portions thereof, the reader can contact roger.traub@downstate.edu.)

The parameters of greatest interest in the RESULTS will be these: which populations of cortical principal cells are electrically coupled; how cortical inhibitory postsynaptic conductances (IPSCs) are scaled; steady depolarizing currents to particular subpopulations of neurons; the properties of AMPA and NMDA conductances at synapses between layer 4 spiny stellate cells; the effects on cortical activity of disconnecting the thalamus.

In vitro experimental methods

Horizontal slices (450 μm thick) were prepared from adult male Wistar rats (150–250 g). Neocortical slices containing primary and secondary auditory regions and secondary parietal regions were maintained at 34°C at the interface between warm wetted 95% O_2-5% CO_2 and artificial cerebrospinal fluid (CSF) containing (in mM): KCl 3; NaH_2PO_4 1.25; $MgSO_4$ 1; $CaCl_2$ 1.2; $NaHCO_3$ 24; glucose 10; NaCl 126. Extracellular recordings from primary auditory cortex were obtained by using glass micropipettes containing artificial CSF (resistance $<$0.5 MΩ). Intracellular recordings were obtained with sharp microelectrodes filled with potassium acetate (resistance 30–90 MΩ), and, in some cases, with the addition of 2% biocytin. For identification of biocytin-filled cells, slices were immediately fixed in 4% paraformaldehyde (PFA) in phosphate-buffered saline, following the recording. Signals were analog filtered at 2 kHz and digitized at 10 kHz. Cells other than those in layer 4 were identified by physiological criteria (regular spiking, fast spiking, intrinsic bursting). Slices were bathed in 400 nM kainate (Tocris, Bristol, UK) and 40 μM picrotoxin (Tocris). In some cases, CGP55845A (10 μM, Sigma-Aldrich UK, Dorset, UK) was added as well, to block $GABA_B$ receptors. All procedures were carried out in accordance with the UK Animals (Scientific Procedures) Act of 1986.

In vivo experimental methods

Experiments were conducted in accordance with the ethical guidelines of the National Institutes of Health and with the approval of the Institutional Animal Care and Use Committee of the University of Pennsylvania. Adult male Sprague–Dawley rats (350–450 g) were anesthetized with pentobarbital (50 mg/kg intraperitoneally). Buprenorphine (0.03 mg/kg subcutaneously) was administered to provide additional analgesia. Animals were paralyzed with gallamine triethiodide and artificially ventilated. End-tidal CO_2 (3.5–3.7%) and heart rate were continuously monitored. Body temperature was maintained at 37°C by servocontrolled heating blanket and rectal thermometer (Harvard Apparatus, Holliston, MA). The depth of anesthesia was maintained by supplemental doses of the same anesthetic to keep a constant heart rate and a constant high-amplitude, low-frequency electroencephalogram (EEG) as recorded from a bipolar electrode inserted into the cortex.

For cortical intracellular recordings, a craniotomy was made to expose the surface of the barrel cortex (1.0–3.0 mm posterior to bregma, 4.0–7.0 mm lateral to the midline). The dura was resected over the recording area and mineral oil was applied to prevent dessication. The stability of recordings was improved by drainage of the cisterna magna, hip suspension, and filling of the holes made for recording with a solution of 4% agar.

Intracellular recordings were performed with glass micropipettes filled with 3 M potassium acetate and DC resistances of 80–90 MΩ. A high-impedance amplifier (band-pass of 0–5 kHz) with active bridge circuitry (Cygnus Technology, Delaware Water Gap, PA) was used to record and inject current into the cells. Data were digitized at 10 kHz and stored on a Nicolet Vision (Nicolet Instrument Technologies, Madison, WI). A computer operating Labview (National Instruments, Austin, TX) was used for the on-line averaging of responses. All data analysis was done off-line using routines written in Igor Pro (Wavemetrics, Lake Oswego, OR).

RESULTS

Persistent gamma oscillation

Persistent, or pharmacologically induced, gamma oscillations occur in in vitro preparations and are called "persistent" because, once initiated, they continue as long as the slice remains healthy (Fisahn et al. 1998). In rat auditory cortex in vitro, kainate-induced gamma oscillations have their maximal amplitude in superficial layers (Cunningham et al. 2004a). Interestingly, two other sorts of in vitro gamma oscillations have maximal amplitude in the superficial layers: interneuron gamma evoked by stimulating metabotropic glutamate receptors, during pharmacological blockade of ionotropic glutamate receptors (Whittington et al. 1995); and thalamically evoked cortical gamma oscillations in thalamocortical slices in vitro (Metherate and Cruikshank 1999). [Not all gamma oscillations in vitro follow this rule, however: when gamma is evoked in somatosensory cortex in vitro, with carbachol plus a low concentration of kainate, then the gamma occurs in all cortical layers, with deep gamma 180° out of phase with superficial gamma (Buhl et al. 1998).]

Our earlier model of auditory cortex kainate-induced persistent gamma (Cunningham et al. 2004a) involved simulations of layer 2/3 only, with RS and FRB pyramidal cells, FS interneurons (basket and axoaxonic), and LTS interneurons. Electrical coupling, between axons, occurred within and between RS and FRB pyramidal cell populations; dendritic electrical coupling occurred between FS interneuron dendrites and between LTS interneuron dendrites. As in earlier models of persistent gamma in hippocampus (Traub et al. 2000, 2003a,b), the superficial neocortical model produced gamma as a result of axonal spiking percolating through the principal cell axonal plexus (in the neocortical case, having such spiking boosted by FRB bursting), with resultant bursts of orthrodromic activation of interneurons, and with the interneurons then interrupting the principal cell somata and axons for some tens of milliseconds, by GABAergic inhibition, thereby producing the gamma period.

Figure 2 demonstrates persistent gamma in a full-thickness model of neocortex (the thalamus being disconnected here), one that includes the cell types of the original superficial cortical model, but many other cell types as well: layer 4 spiny stellates, deep pyramids, deep interneurons. Different bias currents were applied to some of the neurons, particularly to superficial FRB neurons (see legend). (This applies to other simulations as well.) As before (compare Cunningham et al. 2004a), gamma is of highest amplitude in the superficial layers (Fig. 2*A*); and cells in the superficial layers have similar firing patterns to the previous model, and to in vitro experiment: sporadic somatic firing of superficial RS pyramids on a background of rhythmic synaptic potentials (Fig. 2*B*), superficial FRB pyramids discharging on approximately every other burst, superficial FS interneurons (e.g., the basket cell shown in *bottom right panel*) firing on a majority of the gamma waves,

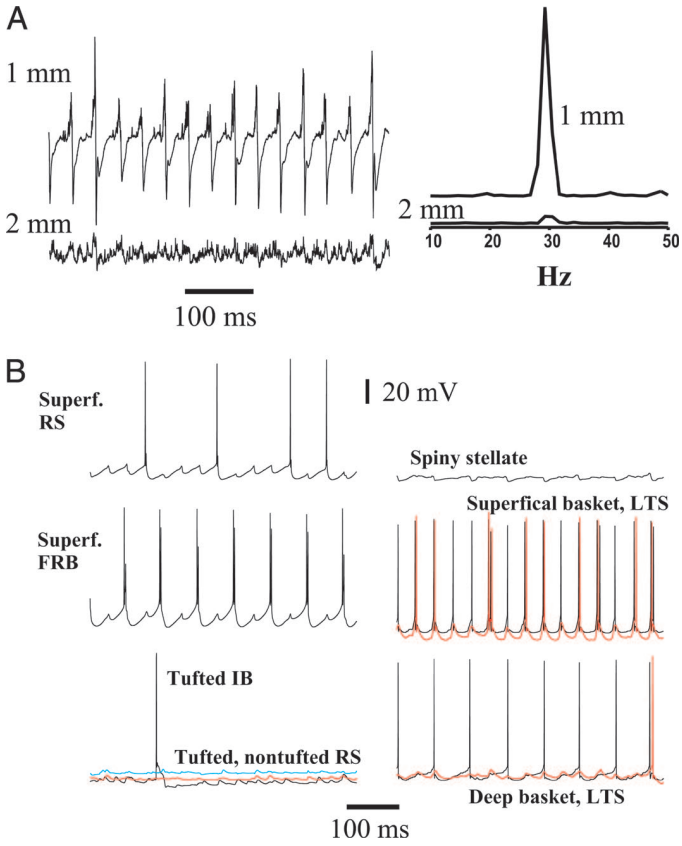

FIG. 2. Simulation of kainate-induced gamma oscillations. *A*: fields in superficial and deep sites, with corresponding power spectra. Note that the oscillations are generated in superficial layers. *B*: firing patterns of selected neurons (compare Cunningham et al. 2004a). (*LTS interneuron traces* are shown in red, *basket cell traces* in black; *tufted RS trace* is blue; *nontufted RS trace* is red.) This simulation was run with inhibitory postsynaptic conductances (IPSCs) 1.25 × baseline, and with "open" axonal gap junctions between cortical principal cells (conductance 4 nS for deep pyramids, and 3 nS for superficial pyramids and spiny stellates). Depolarizing currents were 0.25–0.35 nA for FRB neurons and were <0.1 nA for all other cortical principal cells.

and superficial LTS interneurons firing less than the FS cells. This simulation, however, is not sufficient to explain *why* the deep layers are not generating their own gamma, or at least being driven more strongly by the superficial gamma. The explanation could lie in differences in gap junctional connectivity between the two regions, in properties of interlaminar synaptic connections, in the model's lack of deep FRB neurons, or in other structural features. It is important to note that in vivo (in recordings from cat pericruciate gyri, anterior and posterior suprasylvian areas, and area 18 of the marginal gyrus), gamma oscillations occur in *both* superficial and deep layers with comparable amplitude (Steriade et al. 1996). In addition, FRB cells have been recorded in the infragranular layers of cat pericruciate and suprasylvian gyri (Steriade et al. 1998) and of cat primary visual cortex (J. Cardin and D. Contreras, unpublished data).

Sleep spindles generated in the thalamic network

Individual model thalamic relay cells, and model reticular neurons, fire in bursting and tonic modes, as occurs physiologically (Bal and McCormick 1993; Jahnsen and Llinás 1984a 1984b; Contreras et al. 1993; Deschênes et al. 1984) (APPENDIX A); model thalamic cells can generate rhythmic bursts at approximately 5 Hz during injection of a steady current (not shown). Figure 3 shows a simulated thalamic network spindle and its influence on the cortex. The spindle is initiated by a spontaneous burst in the reticular neurons (Fig. 3*A*). The spindle has a frequency of about 16 Hz (slightly above the frequency range for sleep spindles in cats, but at the upper limit for humans), and has a waxing/waning course (seen in the TCR average in Fig. 3*A*). The relatively fast spindle frequency shown here may be related to the relatively rapid time constants used for the decay of nRT cell-induced $GABA_A$ receptor-mediated IPSCs in TCR cells: 3.3 and 9 ms for the fast and slow components, respectively (APPENDIX B).

Interestingly, the spindle in Fig. 3 stops on its own; in the model case, cessation occurs without time- or calcium-dependent h-current kinetics in TCR neurons (Lüthi and McCormick 1998). Note that individual TCR neurons exhibit the expected sawtooth-like voltage fluctuations (resulting from rebound low-threshold calcium spikes), and each neuron fires on only a fraction of the waves. In contrast, nRT neurons discharge a burst on each spindle wave, as occurs in both in vivo (Contreras et al. 1993) sleep spindles and in vitro (Bal et al. 1995a,b) spindles. The nRT neurons do not, however, show a tonic depolarization as seen in vivo [perhaps attributable in part to persistent g_{Na} (Contreras and Steriade 1993)]; the model nRT neurons instead exhibit the slight tonic hyperpolarization that usually occurs in vitro in ferret slices (Bal et al. 1995a,b). [There are exceptions, however: sometimes nRT neurons in vitro do exhibit an underlying depolarization during a spindle oscillation, sustained by a persistent sodium conductance (Kim and McCormick 1998).] This spindle is generated entirely within the thalamic portion of the model, as corticothalamic excitatory postsynaptic conductances (EPSCs) (AMPA) in TCR (after the initial wave) are at most 0.2 nS.

Figure 3*B* illustrates the effects of the thalamic spindle on spiny stellate neurons: a series of synaptic depolarizations, sometimes with action potentials. Note further the coherent depolarizations in the spiny stellate cells, as shown in the middle trace in Fig. 3*B*, an inverted average of the somatic potentials of all layer 4 spiny stellates; this coherence is aided by the electrical coupling between spiny stellate axons used in the simulation. In addition, a small burst occurs (Fig. 3, *B* and *C*, *); this burst results because of the strong recurrent chemical synaptic excitation between the spiny stellates; when the coupling is weakened 8-fold, the burst does not occur (not shown). Multiphasic waves similar to the asterisk-marked burst in Fig. 3*C*, are on occasion observed in in vivo sleep spindles (Contreras and Steriade 1996; see also Beierlein et al. 2002).

Figure 3*C* shows (*top portion*) that cortical neurons, layer 5 tufted IB pyramids in particular, actually "see," at spindle frequency, a superimposition of synaptic excitation and inhibition; the inhibition results in the model because of strong feedforward excitation of interneurons by thalamic afferents (Swadlow 2003). Trains of IPSPs have been observed experimentally in vivo on the depolarizing phase of the slow oscillation in cortical neurons (Steriade et al. 1993).

Finally, Fig. 3*C* illustrates the behavior of superficial layer 2/3 RS pyramids, including the average of all of the layer 2/3 pyramids (note that the average signal is inverted, so as to approximate a local field potential). During the spindle itself,

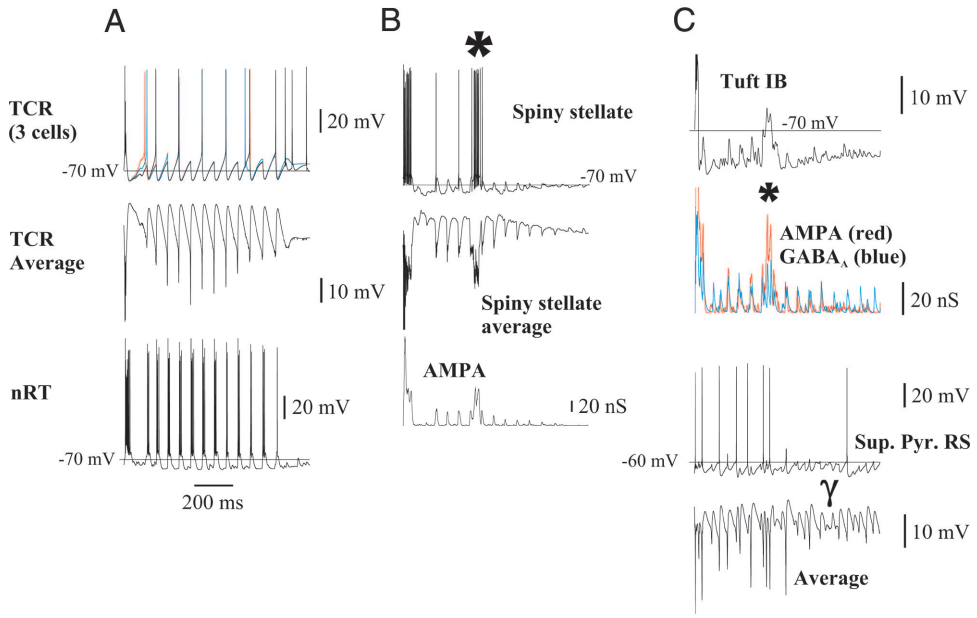

FIG. 3. Simulation of thalamic spindle, with its effects on the cortex. In this case, the corticothalamic input is small [peak α-amino-3-hydroxy-5-methyl-4-isoxazolepropionic acid (AMPA) conductance <0.2 nS in a TCR neuron during the spindle proper, i.e., after the first burst], so that the spindle is generated intrathalamically. Note (*A*) the spindlelike appearance in the mean behavior of thalamic neurons (waxing and waning), the intermittent firing of individual TCR neurons, and the bursting of the nRT cell on each spindle wave. [Compare with, for example, the sleep spindle in a decorticated, ketamine–xylazine anesthetized cat; Fig. 11 of Timofeev and Steriade (1996).] Spindle induces nearly simultaneous excitatory postsynaptic conductances (EPSCs) and IPSCs in cortical neurons (*B*, *C*) by the TCR excitation of both principal cells and interneurons. * marks the occurrence of a small synchronized burst among spiny stellates, dependent on the strong recurrent connections between spiny stellate cells in this simulation; complex synaptic potentials appear in other cortical neurons (e.g., tufted layer 5 IB pyramidal cell in *C*), coincident with the small burst in the spiny stellates. [Note that complex synaptic potentials can sometimes also occur in cortical neurons during in vivo sleep spindles: cf. Fig. 1*A* of Contreras and Steraide (1996).] The spindle is followed by gamma oscillation in superficial layers (*C*, *bottom trace*). Conditions: nRT cells biased by 0.17 to 0.18 nA, and TCR cells by −0.08 to −0.07 nA; axonal gap junction conductance = 3 nS for superficial pyramids and 0 nS for all other cortical principal cells; relative to "baseline conductances" (APPENDIX B), intrinsic nRT γ-aminobutyric acid (GABA) conductances × 0.2; TCR GABA conductances × 3; TCR → nRT AMPA × 3; layer 6 pyramids → nRT *N*-methyl-D-aspartate (NMDA) × 0.02; layer 6 pyramids → TCR NMDA × 0.2 and AMPA × 0.1.

there is a mixture of spindle intervals (about 16 Hz) and gamma intervals (about 30 Hz); gamma is possible in the superficial layers because, in this simulation, superficial pyramids are electrically coupled by their axons. As the spindle ends, gamma alone is present. In vivo as well (in cats) sleep spindles are often followed by a run of gamma oscillation (Steriade et al. 1996), although the gamma in vivo is in both cortex and thalamus. In our model, the gamma is only in the cortex. This difference from in vivo results may arise because the model does not include a mechanism for sustained depolarization of nRT and TCR neurons, such as occurs during the slow oscillation in vivo (Contreras and Steriade 1995; their Figs. 4 and 8), and which may be mediated by metabotropic glutamate receptors (Blethyn et al. 2003; Hughes et al. 2002), and/or by a persistent sodium conductance (Kim and McCormick 1998).

Our simulated spindles require synaptic interactions between nRT and TCR cells. Figure 4 shows that when nRT cells are isolated from other neurons—layer 6 pyramids and TCR neurons—but are not isolated from each other, then there is no spindling, either in the nRT population or elsewhere. (All other parameters in the simulation of Fig. 4 were as for Fig. 3.) Superficial layers (Fig. 4*B*) show continuous gamma oscillations. This model behavior corresponds to the behavior seen with the in vitro ferret slice model of spindles of Bal et al. (1995a,b), but is different from what has been described in vivo, wherein an isolated portion of nucleus reticularis appears to spindle on its own (Steriade et al. 1987). The model as now

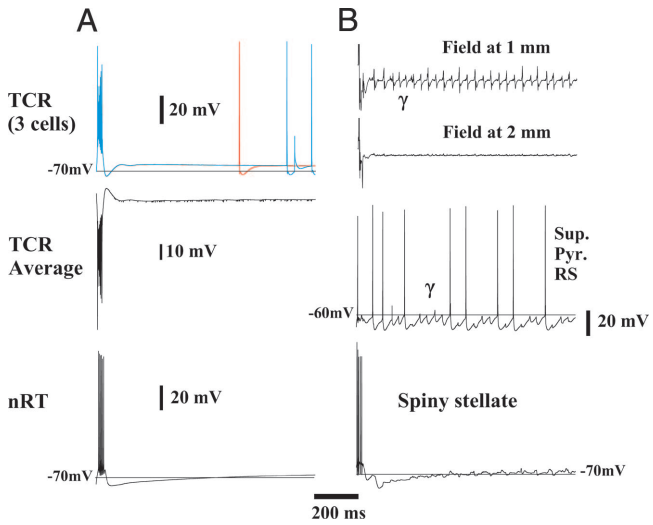

FIG. 4. Under the conditions of Fig. 3, but with nucleus reticularis isolated (i.e., corticoreticular connections are cut, as are connections from nRT neurons to TCR neurons, and vice versa), spindling does not occur. *A*: 3 superimposed TCR somatic voltages, the inverted average of all TCR somatic potentials, and an nRT somatic potential (as in Fig. 3*A*). *B*: cortical field potentials, somatic potential of a superficial RS pyramid and of a layer 4 spiny stellate cell. There are, in this simulation, continuous gamma oscillations in cortical superficial layers (note fields in *B*), reflecting the axonal coupling between pyramidal neurons there. Requirement for nRT/TCR interactions in this model for spindling to occur appears to be similar to in vitro ferret data (von Krosigk et al. 1993), and different from what has been reported for the cat in vivo (Steriade et al. 1987); but see Fig. 5.

constituted appears rather to be consistent with the notion of Ulrich and Huguenard (1997) that within-nRT synaptic inhibition subserves some purpose other than spindling, perhaps what they refer to as "lateral inhibition."

On the other hand, if we repeat the simulation of Fig. 4, isolating the nucleus reticularis, but now (Fig. 5) further depolarize nRT neurons (bias currents in Fig. 4 = 0.17 to 0.18 nA, in Fig. 5 bias currents = 0.27 to 0.28 nA), then a synchronized reticularis oscillation *does* occur (Fig. 5), at approximately 6 Hz. This simulated isolated nRT oscillation requires gap junctions to remain synchronized (Fig. 5*B*), but not within-nRT synaptic inhibition (Fig. 5*C*). Still further depolarization of the nRT neurons in the model resulted in rapid tonic firing; on the other hand, metabotropic effects such as reducing one or more K^+ conductances might have allowed a 10-Hz oscillation, a matter not further explored here. Landisman et al. (2002) observed oscillations in the reticular nucleus in vitro, that required gap junctional communication, but not synaptic transmission; their oscillations could occur at frequencies around 10 Hz. An in vivo study has also found evidence for electrical coupling between nRT neurons, in the form of halothane-sensitive spikelets, and simulations in that study showed that such coupling could contribute to the synchronization of sleep spindle oscillations (Fuentealba et al. 2004).

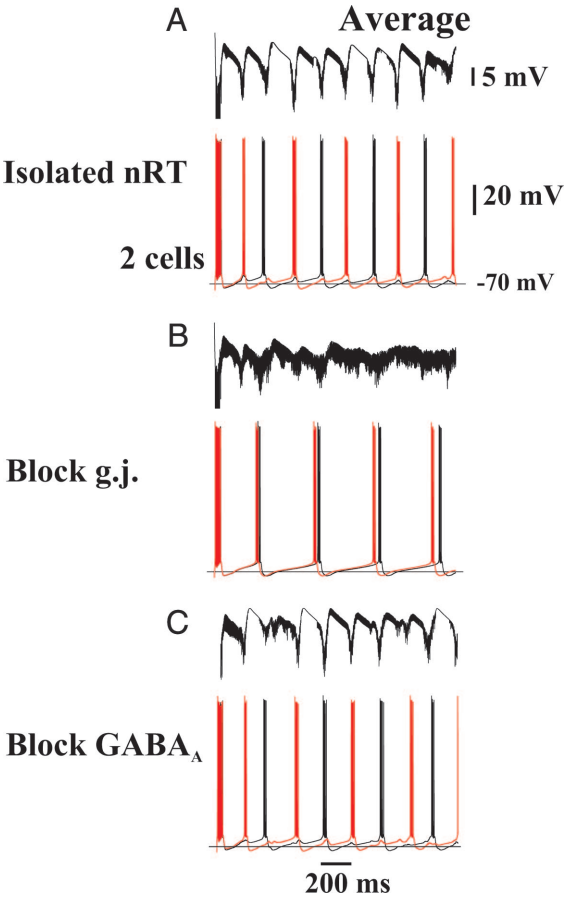

FIG. 5. Depolarization of nRT cells in the isolated model reticular nucleus leads to a 6-Hz synchronized oscillation that requires gap junctions (dendritic in this model, with conductance 1 nS and an average of 2.5 gap junctions on each cell), but that does not require recurrent inhibition. *A*: simulation of Fig. 4 was repeated, but with bias currents to the nRT cells increased by 0.1 nA. There is a 6-Hz population oscillation. *B*: same as *A*, but between-nRT gap junctions were blocked. *C*: same as *A* (with gap junctions intact), but between-nRT synaptic inhibition blocked.

Neocortical epileptogenesis in the presence of electrical coupling between subpopulations of principal neurons

In the monograph of Traub and Miles (1991), some of the basic principles of epileptogenesis in the disinhibited hippocampal CA3 region in vitro were analyzed. CA3 pyramidal cells are intrinsically bursting neurons, and are synaptically connected in such a way that an intrinsic burst in a single presynaptic neuron can evoke, with latency of tens of milliseconds, a burst in a monosynaptically connected postsynaptic neuron (Miles and Wong 1986, 1987). In addition, there is enough recurrent excitatory connectivity, even in vitro, so that on average bursting in one presynaptic neuron will actually evoke bursting in more than one postsynaptic neuron. Thus by a chain reaction, bursting in a single neuron can lead to bursting throughout the whole population, with latency from initial burst to peak number of cells firing dependent on the latency for bursting to spread from cell to cell, and on the density of connections. Although some of the excitatory synaptic connections between neocortical layer 5 tufted pyramids are extremely powerful (see APPENDIX B), we are not aware of data documenting the transmission of a burst from one neuron directly to another in neocortex, either for the case of layer 5 pyramids or for other pairs of neocortical neurons (either of homogeneous cell type or not). Thus it is not clear whether the above analysis of hippocampal bursts applies to cortex. It is certainly the case that during a synchronized burst in neocortex, each principal neuron "experiences" a very large EPSP (Gutnick et al. 1982), consistent with the synchronized discharge of many neurons, although this information is not sufficient to define how the synchrony comes about.

In Traub and Miles (1991), we also considered the case in which a homogeneous population of neurons were all regular spiking, and synaptic connections were not strong enough to transfer firing from a single neuron to another neuron (Fig. 6.11 of that monograph); we asked what sort of stimulus was necessary to synchronize the population. Clearly, firing in a single neuron will no longer suffice. It turns out that a threshold number of cells needs to be discharged together; the value of the threshold number depends on parameters, of course, but in general it can be much smaller than the total number of cells, even if much larger than one. What we did *not* consider at that time, however, was the possibility of electrical coupling between axons (Schmitz et al. 2001), which constitutes another pathway (besides excitatory chemical synapses) whereby action potentials might cross from neuron to neuron.

Because electrical coupling may well occur in neocortex between principal neurons (see APPENDIX B), and because of the heterogeneity of cell types in neocortex, it appears unlikely that an idea as simple as the "chain reaction" (described above) will suffice to capture exactly how synchronization takes place. Therefore what we shall attempt to do in the following is illustrate some examples of what can occur in the model, and make certain correlations with experimental observations. A more theoretical analysis must be deferred.